*Arabian Journal of Chemical and Environmental Research*

*Vol. 09 Issue 02 (2022) 150–167*

# Adsorption of alizarin red S dye from aqueous solution using chemically activated Typha grass (*T. latifolia*): equilibrium, kinetic and thermodynamic studies

**Musa Sani[1], Abdullahi Muhammad Ayuba[1]***

[1]*Department of Pure and Industrial Chemistry, Faculty of Physical Sciences, College of Natural and Pharmaceutical Sciences, Bayero University, PMB 3011, Kano, Nigeria.*

*Received 18 April 2022, Revised 02 Oct 2022, Accepted 08 Oct 2022*

**Abstract**

The adsorption of Alizarin Red S from aqueous solution by base activated typha grass (*T. Latifolia*) (ACT-TG) was investigated in this study using a batch system under controlled conditions. The adsorbent surface was characterized by Fourier transform infrared spectroscopy (FTIR), scanning electron microscopy (SEM) methods and the point of zero charge (PZC). The kinetic data were best described by pseudo-second order models. Adsorption parameters including effect of contact time, adsorbent dosage, initial concentration and pH were studied for optimization purposes and the optimum adsorption capacity was found to be 46.611mg/g. The isotherm for the adsorption processes were also modelled and evaluated and the data generated fitted well the Freundlich isotherm model relative to other models tested. It was estimated through this study that the adsorption rate is positively affected by increase in dose of ACT-TG, dye initial concentration, contact time, pH and temperature. Van't Hoff's plot was used to determine thermodynamic quantities of the adsorption process including ΔS (5.5862J/molK), ΔH (-4.9001kJ/mol) and ΔG (-6.419 to -6.734kJ/mol). The results indicate the adsorption process to be feasible and spontaneous. Therefore, the base activated typha grass can be a potential adsorbent for the removal of hazardous dyes from wastewater.

*Keywords:* Adsorption, Kinetics, Thermodynamic, Isotherms, *T. Latifolia*.

*Corresponding author.
*E-mail address:* ayubaabdullahi@buk.edu.ng

## 1. Introduction

The existence of toxic dyes, heavy metals and other contaminants in a water environment has been attributed to human and industrial activities, which has raised considerable public concern regarding the negative consequences on plants, animals (aquatic and terrestrial) and human lives [1]. However, over a few decades ago, the consciousness of society towards the protection of the environment has infinitely increased. In this regard, the chemical industry has become one of the foremost targets of environmentalists, since its potential adverse impacts can have irreparable damage to the ecosystem. Closely related to the environment is the presence of chemicals, which may seriously jeopardize human health if not treated properly [2].

Dye is a natural or synthetic coloured compound which capacitates to bond chemically with the substrate being applied to it. Dye constitutes a large group of industrial chemicals with over 700,000 tons of waste produced annually [3]. The colorants obtained from plants, minerals or any naturally occurring substances are called natural dyes. Highest percentage of naturally occurring dyes are obtained from plant sources like roots, leaves, bark and wood of trees. Increased demand for readily available, inexpensive, and easily applicable dyes led to the invention and rapid growth of synthetic dyes [4]. Environmental problems caused by the pollution of dyestuffs become more complicated because most of the dyes discharged into the environment are synthetic dyes. With this, a treatment process should be conducted before the wastewater containing dyes are released to the environment [5].

Therefore, this paper is aimed to treat effluent containing Alizarin red S (ARS) dye from aqueous solution using batch adsorption experiments to investigate the effects of operating variables such as contact time, adsorbent dose, initial concentration, pH and temperature.

## 2. Materials and methods

### 2.1 Plant sample collection and preparation

The typha grass was obtained from Marma town, Guri local government area of Jigawa State, Nigeria. The sample was first washed with tap water then distilled water to remove the impurities [6]. The sample was air-dried then oven dried at $105^0$C. The dried sample was pulverized and passed through a 2mm sieve. The sieved sample was activated with 0.5M NaOH in a ratio of 1:20 for 30 minutes as reported by Pandey *et al*. [7].

### 2.2 Preparation of dye solution

The Stock solution of ARS dye was prepared by dissolving exactly weighed 1g of the dye into a 1L to produce 1000 mg/L using distilled water. The experimental solutions of chosen concentration were prepared accordingly by diluting the stock solution with distilled water. The concentration of the un-

adsorbed ARS dye was measured at λmax = 424.89. nm using UV-Visible Spectrometer (Perkin Elmer, Lambda 35).

### 2.3 Characterization of the adsorbent

#### 2.3.1 Scanning electron microscope (SEM)

The surface morphological change of adsorbent sample was investigated using Scanning Electron Microscope (Phenom World Eindhoven). Scanned micrographs of ACT-TG before and after ARS adsorption were taken at an accelerating voltage of 15.00 kV and x500 magnification.

#### 2.3.2 Fourier transform infrared spectroscopy (FTIR)

FTIR analysis of ACT-TG before and after ARS adsorption was carried out using Cary 630 Fourier Transform Infrared Spectrophotometer Agilent Technology. The analysis was done by scanning the sample through a wave number range of 650 – 4000 $cm^{-1}$; 32 scans at $8cm^{-1}$ resolution.

#### 2.3.3 Determination of point of zero charge

Points of zero charge (PZCs) are pH values at which the surface charge components become equal to 0 under given conditions of temperature, applied pressure, and aqueous solution composition [8]. The PZC provides important information about analyte sorption mechanisms. Basically, there are three methods for the determination of point of zero charge namely; (i) Salt addition method (ii) Zeta potential method and (iii) Ion adsorption method.

Salt addition method was employed in this work. PZC values for adsorbents were determined in 0.1 M $NaNO_3$ solution at 303-333K. In this method, 0.2 g of sample was added to 40.0 mL of 0.1 M $NaNO_3$ solution. The pH of the suspension was then adjusted with 0.1 M HCl and 0.1 M NaOH 0.1 using pH-meter (MP 220) to obtain an initial pH value of 2, 4, 6, 7, 8, 10 and 12. Each flask was then vigorously agitated in a shaker bath for 24 h. After settling, the final pH of each suspension was measured very carefully. The ΔpH (the difference between final and initial pH) values were then plotted against the initial pH values [9]. The initial pH at which ΔpH is zero was taken to be the PZC [10].

### 2.4 Batch adsorption

Batch experiments were carried out to determine the optimum conditions for the equilibrium adsorption of ARS onto ACT-TG by adding 0.02g of it with a $20cm^3$ of 50ml initial concentration. The results attained after the optimization experiments were used to conduct the batch adsorption experiments. Each of these systems were separately run in a 250 $cm^3$ conical flask differently at 30, 40, $50^0C$ respectively.

The conical flasks were covered during the equilibration period and placed on a temperature-controlled tightly Innova 4000 incubator shaker for the earlier reported period. After reaching adsorption equilibrium, the content was filtered through Whatman No 1 filter paper. The filtrate was analyzed using Perkin-Elemer Uv-visible spectrophotometer at maximum absorbance wavelength of 424.89nm. The extent of adsorption was calculated using equations (1) and (2) respectively.

$$\text{Adsorption Capacity } (q_e) = \frac{(Co-Ce)x\,V}{m} \quad (1)$$

$$\%\ \text{adsorption} = \left(\frac{Co-Ce}{Co}\right) \text{x } 100 \quad (2)$$

Where qe is the adsorption capacity (mg/g), *Co* and *Ce* are the initial and final equilibrium concentration (mg/l) of Alizarin Red S in solution, V is the volume of Alizarin Red S in solution (L), and *m* is the mass (g) of the adsorbent [11, 12].

## 3. Results and discussion

### 3.1 Fourier transform infrared spectroscopy (FT-IR)

The FTIR spectra of the adsorbent before and after adsorption onto ARS are presented in Figure 1. The FTIR spectra of ACT-TG with loaded ARS equivalents are shown in **Figure 1**. Peaks were observed at 3320, 2914 1600, 1510 and 1104 $cm^{-1}$ in ACT-TG before adsorption, which were attributed to O-H stretching, C-H stretching, C=O stretching and C=C stretching respectively [13, 14]. The free O–H stretch for ACT-TG appeared before adsorption at 3320$cm^{-1}$. After loading ACT-TG with ARS there was a shift in the vibration frequency of the free O–H stretch. This shift in the vibration frequencies might be due to binding of toxic ions onto the surface of the adsorbents [15]. However, The FTIR spectrum after adsorption also shows other shifted peak positions and appearance of some new peaks indicating interactions between the adsorbents and adsorbates. Furthermore, the presence of hydroxyl group and carbonyl group is attributed to the presence of carboxylic acids group present in the adsorbents. The hydroxyl, carboxyl and carboxylic acid are important adsorption sites [3].

### 3.2 Scanning electron microscope (SEM)

The SEM micrographs of the ACT-TG before and after adsorption of ARS are presented in **Figure 2**. However, the machine was operated at an accelerating voltage of 15.00 kV and at magnification between 300-1000. The scanned micrographs of ACT-TG before adsorption shows a moderately rough surface which is characterized with defects made of cracks and holes and it might due to the presence of adhering particles which may be dust or other impurities [16].

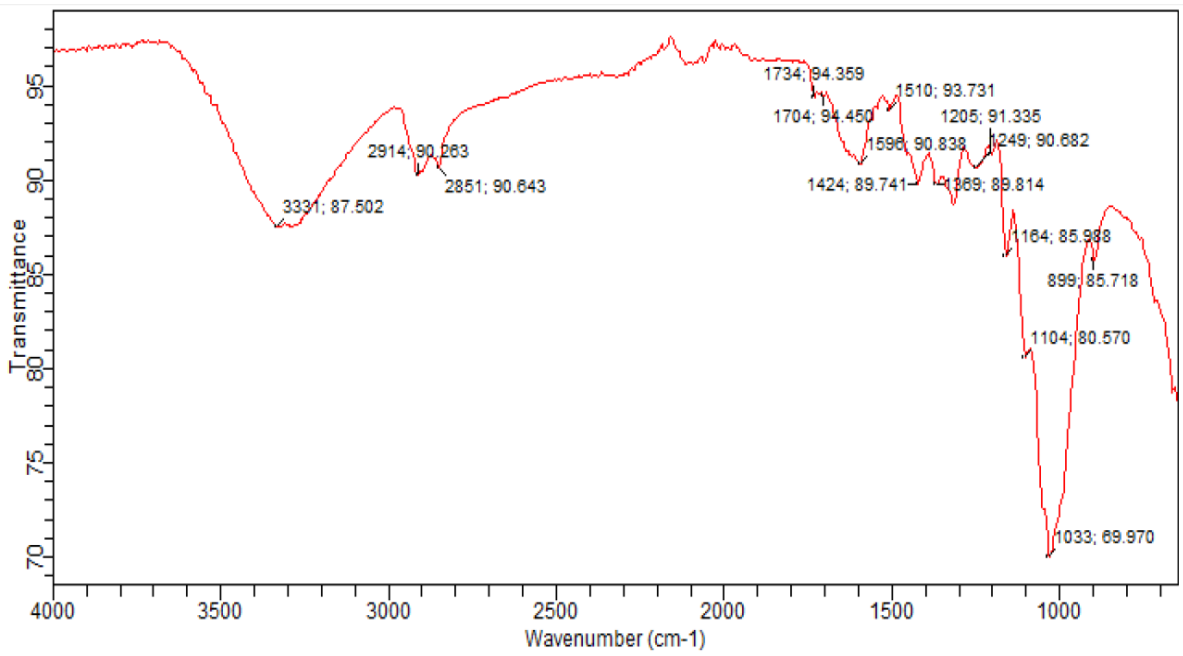


**(a)**

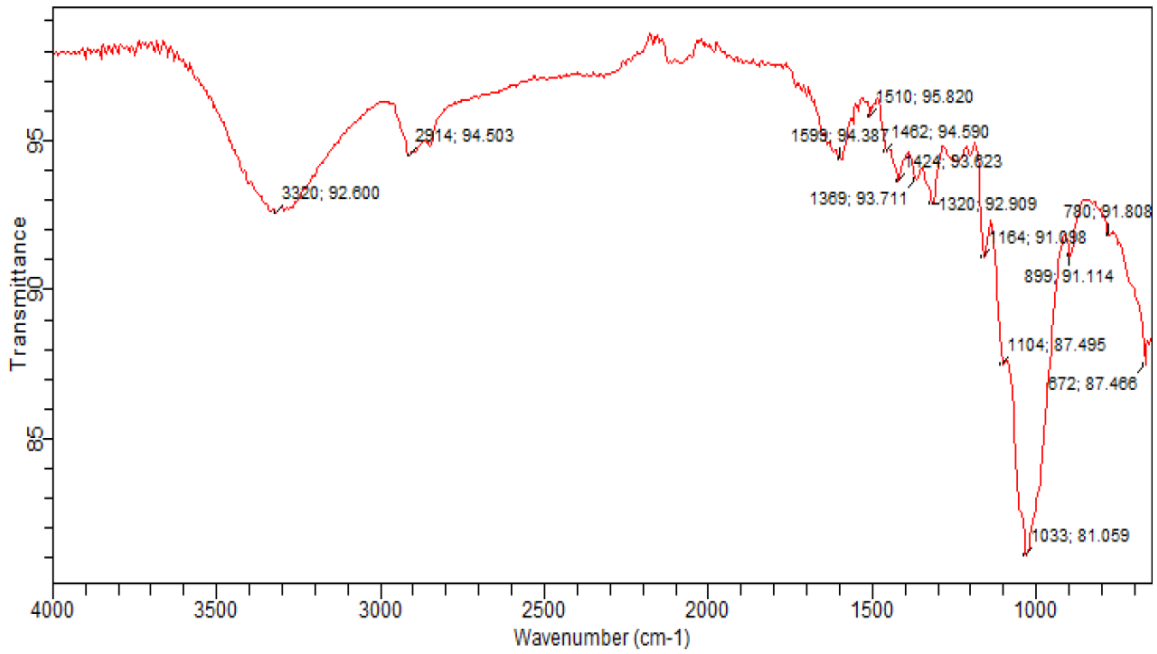


**(b)**

**Figure 1**. FTIR spectral of ACT-TG (a) before and (b) after adsorption onto ARS

**Table 1.** Different functional group recognized before and after adsorption of ARS onto ACT-TG

| Functional group | Absorption range ($cm^{-1}$) | Before absorption ($cm^{-1}$) | After absorption onto ARS ($cm^{-1}$) | Difference ($cm^{-1}$) |
|---|---|---|---|---|
| OH stretch | 3700-2500 | 3320 | 3331 | 11 |
| C-H stretch | 3000-2840 | 2914 | 2914 | 0 |
| C=O stretch | 1710-1580 | 1600 | 1704 | 104 |
| C≡C stretch | 1675-1550 | 1510 | 1510 | 0 |
| C-O stretch | 1080-1300 | 1104 | 1104 | 0 |

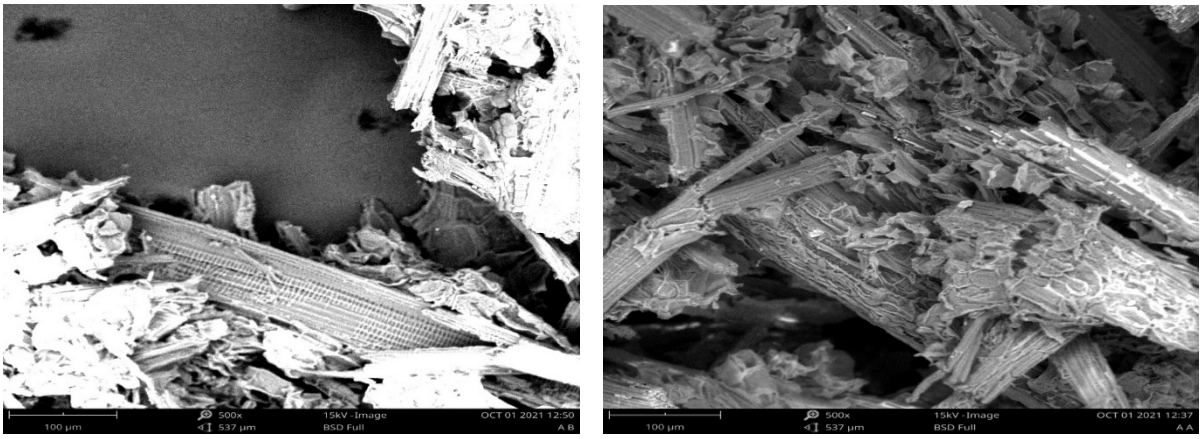

**(a)** **(b)**

**Figure 2.** SEM Micrograph of ACT-TG (a) before and (b) after adsorption of ARS

### 3.3 Determination of point of zero charge

The point of zero charge (PZC) result for ACT-TG adsorbent is presented in **Figure 3**. The PZC studied is around 7, which indicate the presence of perfect charge balance on the surface of the adsorbent within the equilibrated ions in an aqueous solution. Moreover, Substrates with low PZC values show the highest tendency to treat effluents contaminated with cations, while substrates with high PZC values would be more appropriate to capture anions. The magnitude of the surface charge depends on the abundance and types of functional groups present, and on the pH of the solution [17].

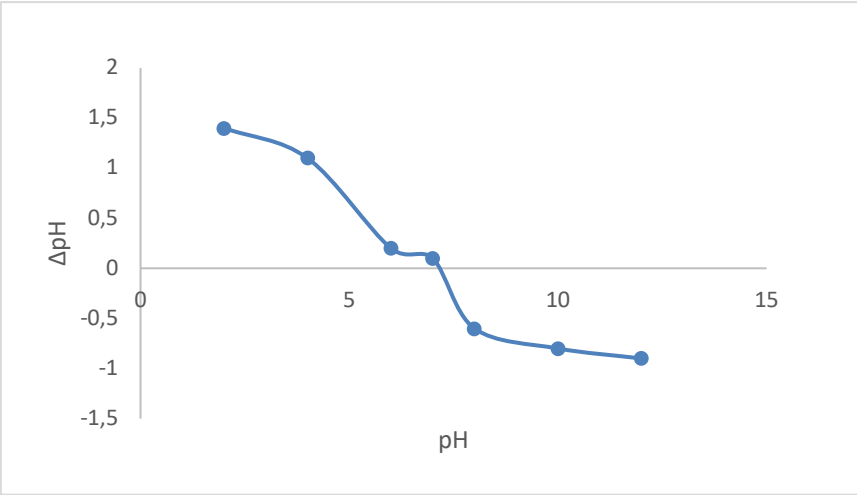


**Figure 3.** Point of Zero Charge (PZC) of ACT-TG

### 3.4 Batch adsorption

#### (a) Effect of contact time

**Figure 4a** showed deviation of the amount of ARS adsorbed with time onto ACT-TG. From the plot, it is obvious that the rate increased rapidly with time, and then reached equilibrium at 30 mins. The adsorption capacity and percentage removal of ARS onto the adsorbent significantly increased during

the initial adsorption stage, and then equilibrium was nearly reached. At this time, removal efficiency of ARS was 9.52 mg/l. Hence, in this current work, 30 min was chosen as the equilibrium time. However, the removal rate of adsorbate was rapid initially, but it gradually decreases with time until it reaches equilibrium. This can be due to the fact that a large number of vacant surface sites are available for adsorption at the initial stage, and after a lapse of time, the remaining vacant surface sites are not easy to be occupied due to repulsive forces between the solute molecules on the solid and bulk phases. Similar findings were reported by other authors [18].

**(b) Effect of adsorbent dose**

**Figure 4b** represents the profile diagram of the doses for ACT-TG used for the removal of ARS. The adsorption capacity of ARS onto ACT-TG decreased with increasing adsorbent dose as per 47.59 $mgg^{-1}$ down to 4.76 $mgg^{-1}$, as the dose of adsorbent increased within range of 0.02g– 0.2g. Thus, 0.02g dose of the adsorbents was obtained as the optimum [19]. However, it was observed that the efficiency of the removal of ARS increases significantly as adsorbent dose increases. The effect of dose of adsorbent on the removal of ARS dye onto ACT-TG is shown in **Figure 4b**. The graph indicates that 0.02g of ACT-TG leads to the removal of 96.2% of ARS. It is evident from the plot that already 0.02g of ACT-TG leads to virtually quantitative removal of a maximum adsorption capacity of 47.59 $mgg^{-1}$ of ARS [20].

**(c) Effect of initial concentration**

**Figure 4c** revealed the plot showing the effect of initial dye concentration on the adsorption of ARS onto ACT-TG. It was detected that the total volume of ARS adsorbed per gram of the adsorbent increased with increasing concentration. At low concentration, the available driving force for transfer of ARS onto ACT-TG particles is low, while at high concentration, there is a corresponding increase in the driving force, thereby improving the interaction between the ARS dye in the aqueous phase and the active sites of the adsorbent [21].

**(d) Effect of pH**

**Figure 4d** shows the effect of pH on the adsorption of ARS onto ACT-TG. Basic pH had an effective influence on the acceptance of ARS increasing the pH from 2 toward 10, the uptake capacity of the adsorbent increased up to pH 7. The maximum adsorption of ARS dye by ACT-TG happened at pH 7, leading to 47.76mg/g. This outcome can be due to the change in surface charge of the activated carbon [22]. However, it was observed that the lowest uptake capacity was determined at pH 4 while its climax was determined at pH 7 [6].

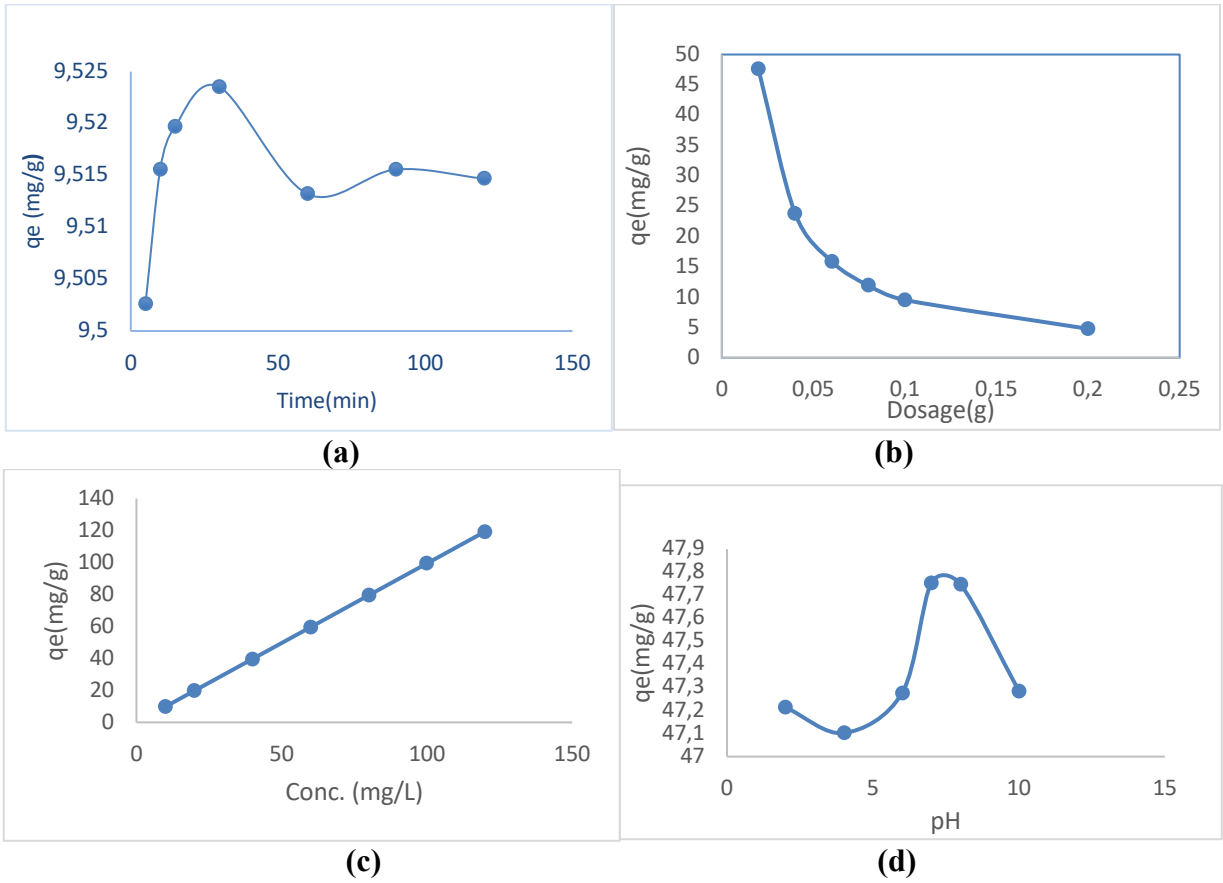


**Figure 4**. (a) Effect of contact time (b) Adsorbent Dosage (c) Initial Concentration (d) pH on the Adsorption of ARS onto ACT-TG

### 3.5 Adsorption kinetics

The kinetic studies are useful to provide information about uptake rate, which gives important information for designing and modelling the adsorption processes [23]. The data generated during batch adsorption experiments when samples were withdrawn at 10 minutes' interval for a maximum period of 120 minutes was imperilled to different kinetic models. This is with an aim of possibly establishing the mechanism of the interaction of the dye with the surface of the adsorbent (ACT-TG). The following models were tested, reported and discussed.

#### (a) The pseudo first-order equation

The pseudo first-order equation is generally expressed as follows [24]:

$$\frac{dq_t}{dt} = k_1(q_e - q_t) \qquad (3)$$

Where: $q_e$ and $q_t$ are the adsorption capacity at equilibrium and at time t, respectively ($mg.g^{-1}$), $k_1$ is the rate constant of pseudo first-order adsorption ($l.min^{-1}$). After integration and applying boundary conditions t = 0 to t = t and $q_t = 0$ to $q_t = q_t$, the integrated form of Eq. (3) becomes:

$$\log(q_e - q_t) = \log(q_e) - \frac{k_1}{2.303}t \qquad (4)$$

The values of log ($q_e$ - $q_t$) were linearly correlated with t. The plot (**Figure 5a**) of log ($q_e$ - $q_t$) vs. t should give a linear relationship from which $k_1$ and $q_e$ can be determined from the slope and intercept of the plot respectively.

**(b) The pseudo second-order equation**

Kinetic rate equation for the pseudo second-order adsorption is expressed as:

$$\frac{dq_t}{dt} = k_2(q_e - q_t)^2 \quad (5)$$

The pseudo second-order adsorption rate constant is $k_2$ (g.mg$^{-1}$min$^{-1}$). For the boundary conditions t = 0 to t = t and $q_t$ = 0 to $q_t$ = $q_t$, the integrated form of Eq. (5) becomes:

$$\frac{1}{(q_e - q_t)} = \frac{1}{q_e} + K_t \quad (6)$$

Equation (6) rearranged to obtain Eq. (7), a linear form:

$$\frac{t}{q_t} = \frac{1}{K_2 q_e^2} + \frac{1}{q_e}(t) \quad (7)$$

The initial adsorption rate, h (mg.g$^{-1}$min$^{-1}$) is;

$$h = K_2 q_e^2 \quad (8)$$

Then equation (8) becomes

$$\left(\frac{t}{q_t}\right) = \frac{1}{h} + \frac{1}{q_e}(t) \quad (9)$$

The plot of ($t/q_t$) against t of Eq. (9) give a linear relationship from which $k_2$ and $q_e$ can be obtained from the intercept and slope of the plot respectively (**Figure 5b**).

**(c) Elovich equation**

The Elovich kinetic model is defined by the following relation [25].

$$q_t = {}^{1}/_{\beta} \ln(\alpha\beta) + \left({}^{1}/_{\beta}\right) lnt \quad (10)$$

This model gives useful information on the extent of both surface activity and activation energy for adsorption process. The parameters *(α)* and *(β)* was calculated from the slope and intercept of the linear plot of *q*t versus ln (t) (**Figure 5c**).

**(d) Intraparticle diffusion equation**

The slowest step in an adsorption process is usually taken as the rate determining step. This step is often attributed to pore and intra particle diffusion. Since pseudo first and pseudo second order models cannot provide information on effect of intra particle diffusion in adsorption, intra particle diffusion model can

be used. Possibility of involvement of intra particle diffusion model as the sole mechanism was investigated according to Weber–Moris equation (11) [12, 26].

$$q_t = C + K_{int} t^{1_2} \quad (11)$$

Where the constant $k_{int}$ (mg/g $min^{0.5}$) is the intra particle diffusion rate and *C* is the boundary layer thickness.

**Table 2.** Kinetic models for the adsorption of ARS onto ACT-TG

| Kinetic Models | Parameters | | | |
|---|---|---|---|---|
| Pseudo-first order | $qe_{Cal}$(mg/g) | $qe_{Exp}$(mg/g) | $k_1$($min^{-1}$) | $R^2$ |
| | 47.507 | 0.968 | 0.00004 | 0.0698 |
| Pseudo-second order | $qe_{Cal}$(mg/g) | $qe_{Exp}$(mg/g) | $k_2$($min^{-1}$) | $R^2$ |
| | 47.507 | 46.611 | 1.540 | 0.9990 |
| Elovich | B | A | | $R^2$ |
| | -3.853 | -8.758 | | 0.4241 |
| Intraparticle | $k_3$ | C | | $R^2$ |
| Diffusion | -0.029 | 47.139 | | 0.3471 |

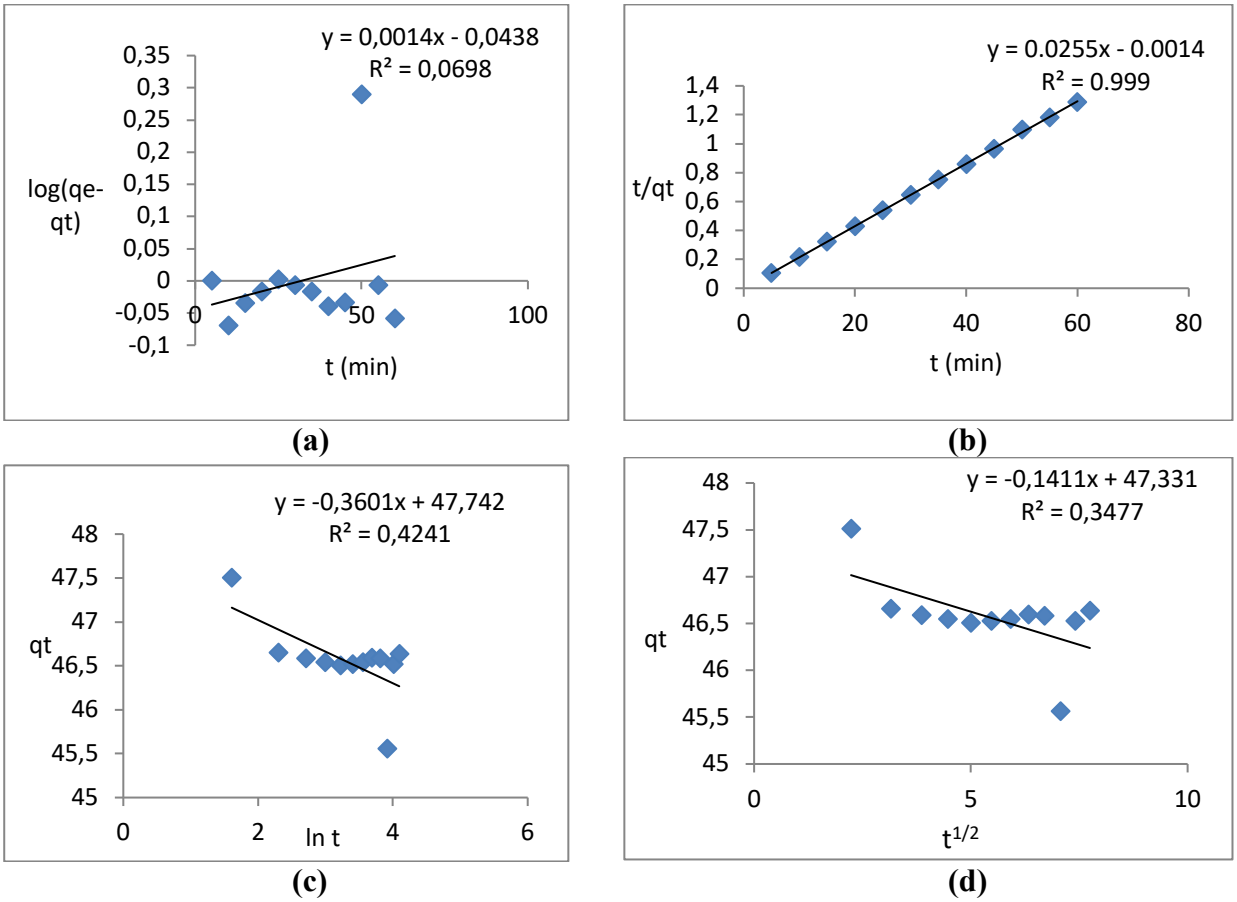


**Figure 5.** Adsorption Kinetics of (a) pseudo first order (b) pseudo second order (c) Elovich (d) Intraparticle diffusion of ARS onto ACT-TG

If the rate-limiting step is only due to the intra particle diffusion, then *qt* versus $t_{1/2}$ will be linear and the plot passes through the origin (**Figure 5d**). **Table 2** shows the constants obtained from the tested kinetic

models for the adsorption of ARS onto ACT-TG. The pseudo-second-order kinetic model support the experimental data quite well; the correlation coefficient values, $R^2$, is close to unity, the theoretical and experimental uptakes are in well in agreement. This gives the applicability of the second-order kinetic model to report the adsorption process of ARS onto the adsorbent, ACT-TG.

### 3.6 Adsorption isotherms

The relationship between the equilibrium concentration of the adsorbate in the liquid phase and in the solid phase adsorbent were subjected into four adsorption isotherm equations. More importantly, to determine which of the isotherms best describes the adsorption process. Experimental data were substituted into the equations and appropriate graphs, constants and other variables were generated for each of the following equations:

**(a) Langmuir isotherm**

This report quantitatively describes the formation of a monolayer adsorbate on the surface of the adsorbent, without further adsorption taking place. So, the Langmuir stands in the place of equilibrium distribution of dye molecules between the solid and liquid phases [27]. Langmuir signified the following equations:

$$q_e = \frac{Q_{OK_lC_e}}{1 + K_lC_e} \quad (12)$$

Langmuir adsorption parameters were obtained by converting the Langmuir equation (12) into linear form.

$$\frac{1}{q_e} = \frac{1}{Q_o} + \frac{1}{Q_oK_lC_e} \quad (13)$$

Where: $C_e$= the equilibrium concentration of adsorbate ($mg.l^{-1}$), $q_e$ = the amount of dye adsorbed per gram of the adsorbent at equilibrium ($mg.g^{-1}$), $Q_o$= maximum monolayer coverage capacity (mg.g-1), $K_l$= Langmuir isotherm constant ($L.mg^{-1}$).

The values of $q_{max}$ and $K_l$ were computed from the slope and intercept of the Langmuir plot of $\frac{1}{qe}$ versus $\frac{1}{Ce}$ (**Figure 6a**) [28]. The essential features of the Langmuir isotherm may be expressed in terms of equilibrium parameter $R_L$, which is a dimensionless constant referred to as separation factor or equilibrium parameter [29].

$$R_L = \frac{1}{(1 + K_lC_o)} \quad (14)$$

Where: Co = initial concentration, $K_l$ = the constant related to the energy of adsorption (Langmuir constant). $R_L$ value indicates the adsorption nature to be either unfavorable if $R_L>1$, linear if $R_L=1$, favorable if $0<R_L<1$ and irreversible if $R_L= 0$.

**(b) Freundlich isotherm**

This is commonly used to describe the adsorption characteristics for the heterogeneous surface [30]. The equation proposed by Freundlich is as presented in equation (15):

$$Q_e = K_f C_e^{1/n} \quad (15)$$

Where $K_f$ = Freundlich isotherm constant ($mg.g^{-1}$), n = adsorption intensity, Ce = the equilibrium concentration of adsorbate ($mg.L^{-1}$), Qe = the amount of metal adsorbed per gram of the adsorbent at equilibrium ($mg.g^{-1}$). Changing equation (15) to linear form, give:

$$LogQ_e = logK_f + \frac{1}{n} logC_e \quad (16)$$

Where Ce is the equilibrium concentration of adsorbate (mg/L), qe is the amount of ARS adsorbed per gram of the adsorbent at equilibrium (mg/g). The plotting of logQe versus logCe gave a graph presented in **Figure 6b** and the values of $K_f$ and n were calculated and tabulated in **Table 3**.

**(c) Temkin isotherm**

This is categorised by binding energies which is uniform distribution up to the climax of binding energy [31.32]. The linear equation of this isotherm is represented in Equation. (17):

$$q_e = B_T lnC_e + B_T lnK_T \quad (17)$$

$$B_T = RT/b_T \quad (18)$$

**Figure 6c** shows the Temkin model plots for the adsorbate adsorption onto ACT-TG. From **Table 3**, the $B_T$ (energy of adsorption) value was found to be 36.188 while $A_T$ (equilibrium binding energy) value is 0.934 L $mg^{-1}$. Therefore, adsorption rate of ARS molecules is bonded to the sites of ACT-TG as indicated in **Table 3**.

**(d) Dubinin-Radushkevich (D-R)**

Dubinin–Radushkevich isotherm is an empirical model initially conceived for the adsorption of subcritical vapours onto micro pore solids following a pore filling mechanism [33]. The linear form of Dubinin-Radushkevich (D-R) isotherm model is given by equation (19):

$$lnq_e = lnq_m - \beta\varepsilon^2 \quad (19)$$

$$\varepsilon = RTln\,[1 + 1/Ce] \quad (20)$$

$$E = 1/\sqrt{2\beta} \quad (21)$$

**Figure 6d** presents the plot of $lnq_e$ versus $\varepsilon^2$. The mean free energy (E) obtained from Dubinin-Rudushkevich (D-R) model provides information about chemical or physical properties of the adsorption process [34]. The D-R correlation coefficient is the lowest ($R^2$) as observed from **Table 3** in comparison with all the studied isotherms. Thus, the D-R model exhibited less fit with the experimental data. The E value was less than 8 kJ $mol^{-1}$ implying that the adsorption process is controlled by physical forces [35].

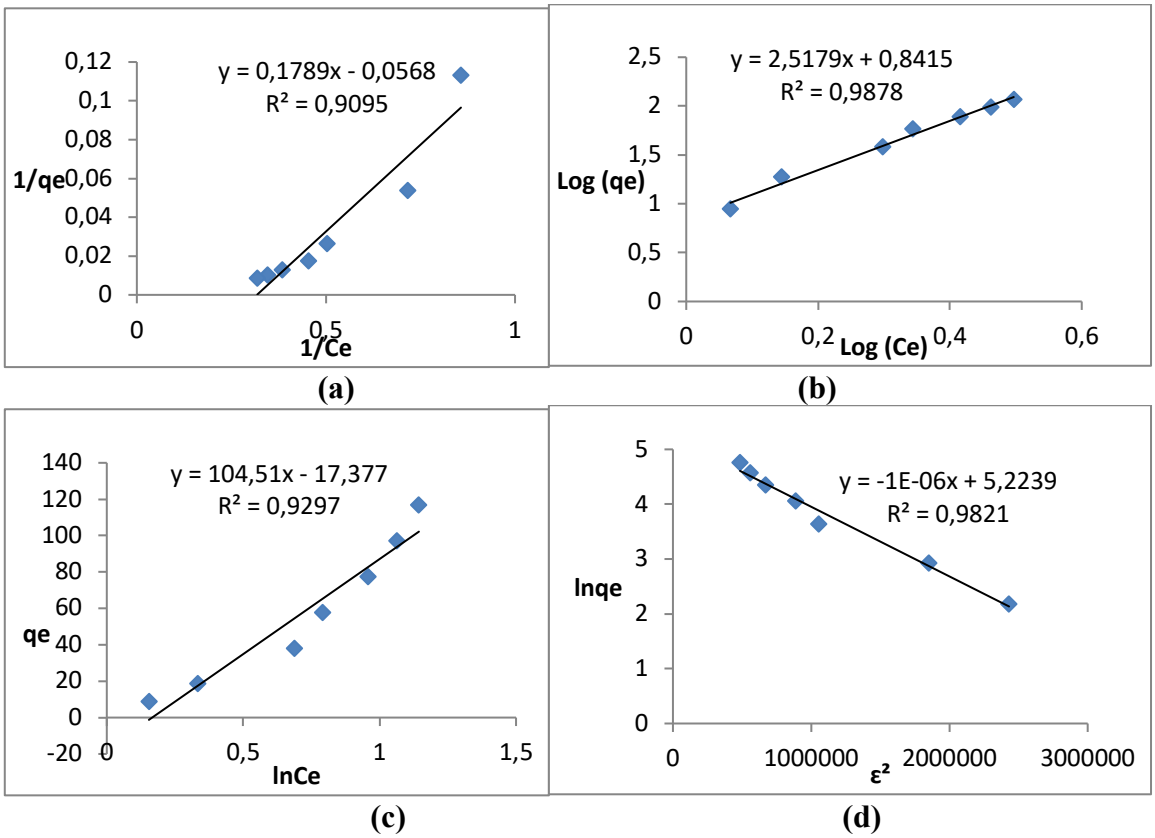


**Figure 6.** Adsorption isotherms plots Langmuir (a) Freundlich (b) Temkin (c) Dubinin-Radush-kevich for the adsorption of ARS onto ACT-TG

**Table 3.** Adsorption Isotherm constants for the adsorption of ARS onto ACT-TG

| Parameter | Alizarin Red S |
|---|---|
| Langmuir | |
| $Q_O$(mg/g) | 17.605634 |
| $K_L$(L/mg) | 0.317496 |
| $R_L$ | 0.0498759 |
| $R^2$ | 0.9095 |
| Freundlich | |
| 1/n | 1.6757 |
| n | 0.596766 |
| $K_F$ | 9.418896 |
| $R^2$ | 0.9878 |
| Temkin | |
| $A_T$ | 0.934 |
| $B_T$ | 36.188 |
| B | 69.614 |
| $R^2$ | 0.9297 |
| Dubinin-Radushkevich | |
| $q_m$(mg/g) | 119.414 |
| $K_{dr}$(mol$^2$/kJ$^2$) | $1.0\times10^{-6}$ |
| E(kJ/mol) | 0.707 |
| $R^2$ | 0.9821 |

### 3.7 Thermodynamic studies

The influence of temperature on Alizarin Red S adsorption onto ACT-TG was determined by changing the temperature from 30°C to 50°C (303 -323K) and by keeping all factors (contact time, pH, adsorbent dose, agitation speed and initial ARS concentrations) at optimized values. The thermodynamic parameters such as changes in free energy (ΔG), enthalpy (ΔH) and entropy (ΔS) were determined to ascertain the feasibility and spontaneous nature of the adsorption process using equations (22), (23) and (24):

$$\Delta G = -RT\ln K_L \quad (22)$$

$$\Delta G = \Delta H - T\Delta S \quad (23)$$

Where R is the gas constant (8.314 J/molK), T is the absolute temperature (K), and $K_L$ is the thermodynamic equilibrium constant,

Combining equations (22) and (23) we got equation (24)

$$\ln K_L = -\frac{\Delta H}{RT} + \frac{\Delta S}{R} \quad (24)$$

The plot of $\ln K_L$ (L/mol) versus 1/T (Van't Hoff) gave values of ΔH and ΔS calculated from the slope and intercept of the plot, and $K_L$ is equal to qe/Ce obtained at different temperatures [35].

**Table 4**. Thermodynamic parameters for the adsorption of Alizarin Red S onto ACT-TG

| T (K) | $K_L$ | ΔG (kJ/mol) | ΔH (kJ/mol) | ΔS (J/mol.K) |
|---|---|---|---|---|
| 303 | 13.841 | -6.419 | -4.9001 | 5.5861766 |
| 313 | 12.593 | -6.592 | | |
| 323 | 12.279 | -6.734 | | |

The negative value of the Gibbs free energy (ΔG) in **Table 4**, suggests that the ARS removal process is thermodynamically feasible and spontaneous. The increase in the negative value at elevated temperatures indicates that the adsorbate uptake by ACT-TG is improved at higher temperatures in the studied range. The negative value of the enthalpy change (ΔH) implies the exothermic nature of the adsorption process. The extent of enthalpy change (ΔH) may provide an insight about the kind of adsorption process involved. If the value of ΔH is greater than 80 kJ/mol, the process is chemisorption which involves chemical bonding between the adsorbate and adsorbent surface. On the other hand, when ΔH is lower than 80 kJ/mol, it signifies the adsorption process is physisorption [36].

## Conclusion

Base activated typha grass adsorbent was prepared and used to remove Alizarin Red S dye from aqueous solution through a batch adsorption technique. The adsorbent was first characterized using FTIR, SEM and PZC methods. Adsorption isotherm models employed to study the adsorption data obtained were

Langmuir, Freundlich, Temkin and Dubinin-Radushkevich. The data obtained indicated Freundlich to be the most favourable isotherm. Out of the four kinetic models tested, pseudo second order kinetics was found to fit well the kinetic data generated. The adsorption process was qualified to be spontaneous and feasible based on the thermodynamic parameters calculated including enthalpy, entropy and Gibb's free energy. On the basis of the results obtained, it can be concluded that base activated typha grass can efficiently be utilized as an adsorbent for the removal of Alizarin Red S dye from aqueous solution at the studied conditions through the mechanism of physical adsorption. As a waste product, it provides solution for solid-waste management and solves the problem of its disposal and therefore, the reported study is an environmentally friendly method. For future studies, the usability of activated typha grass for dyes removal from real wastewater should be studied and as comparison, a fixed bed column be employed to investigate the effect of reactor design.

**Conflict of Interest**

The authors declare that the research was conducted in the absence of any commercial or financial relationships that could be construed as a potential conflict of interest.

**References**

[1] A. Hamzezadeh, Y. Rashtbari, S. Afshin, M. Morovati, M. Vosoughi, Application of low-cost material for adsorption of dye from aqueous solution. *International Journal of Environmental Analytical Chemistry*, 102(1): 254-269 (2022).

[2] X. You, R. Zhou, Y. Zhu, D. Bu, D. Cheng, Adsorption of dyes methyl violet and malachite green from aqueous solution on multi-step modified rice husk powder in single and binary systems: Characterization, adsorption behavior and physical interpretations. *Journal of Hazardous Materials*, 430*:*128445 (2022).

[3] U. Itodo, A. Usman, C. Ugboaja, A Rate Study of Received and Derived Activated Carbon and Pseudo Constants for Methyl Red Sorption. *Journal of Encapsulation and Adsorption Sciences*, 1:57- 64 (2011).

[4] V. Laxmi, Removal of malachite green dye from water using orange peel as an adsorbent. Master of Technology Dissertation, National Institute of Technology, India (2014).

[5] J. N. Putro, J. Yi-Hsu, E. S. Felycia, P. S. Shella, I. Suryadi, Biosorption of dyes'' *Green Chemistry and Water Remediation.* 5(3):67-84 (2021). https://doi.org/10.1016/B978-0-12-817742-6.00004-9

[6] F. O. Nwosu, F. A. Adekola, A. O. Salami, Adsorption of N-nitrophenol (PNP) Using Pilli nut shell action. *Pak. J. Anal. Environ. Chem.* 18 (1): 69 (2017).. https://doi.org/10.21743/pjaec/2017.06.07

[7] R. Pandey, Utilization of NaOH modified *Desmostachya bipinnata* (Kush grass) leaves and *Bambusa*

*arundinacea* (bamboo) leaves for Cd (II) removal from aqueous solution. *J. Environ. Chem. Eng*. 3 (1): 593–602 (2018).

[8] A. Villabona-Ortíz, K. J. Figueroa-Lopez, R. Ortega-Toro, Kinetics and Adsorption Equilibrium in the Removal of Azo-Anionic Dyes by Modified Cellulose. *Sustainability*, 14(6): 3640 (2022).

[9] S. N. Guilhen, T. Watanabe, T. T. Silva, S. Rovani, J. T. Marumo, J. A. S. Tenório, O. Mašek, L. G. de Araujo, Role of Point of Zero Charge in the Adsorption of Cationic Textile Dye on Standard Biochars from Aqueous Solutions: Selection Criteria and Performance Assessment. *Recent Progress in Materials*, 4(2) (2022). doi:10.21926/rpm.2202010.

[10] K. Hassen, G. Boczkaj, I. Ghorbel-Abid, M. Trabelsi-Ayadi, Determination of phenylbutazone, sulfamethazine, carbendazim and linuron using a novel pine bark biosorbent for solid-phase extraction (SPE) with high-performance liquid chromatography (HPLC). *Instrumentation Science & Technology,* 1-13 (2022).

[11] A. M. Ayuba, B. Idoko, Kinetic, equilibrium and thermodynamic studies on the adsorption of crystal violet dye from aqueous solution using activated cowpea (*Vigna Unguiculata)* husk. *Applied Journal of Environmental Engineering Sciences,* 6(2): 182-195 (2020).

[12] A. M. Ayuba, B. Idoko, Cowpea husk adsorbent for the removal of crystal violet dye from aqueous solution. *Arabian Journal of Chemical and Environmental Research* 08(01): 114–132 (2021).

[13] H. Ali, N. Mladenka, I. Mihajlović, Sorption of carbendazim and linuron from aqueous solutions with activated carbon produced from spent coffee grounds: Equilibrium, kinetic and thermodynamic approach. *Journal of Environmental Science and Health*, Part B, doi: 10.1080/03601234.2018.1550307 (2018).

[14] A. A. Werkneh, N. G. Habtu, H. D. Beyene, Removal of Hexavalent Chromium from Tannery Wastewater using Activated Carbon Primed from Sugarcane Bagasse: Adsorption/Desorption Studies. *American Journal of Applied Chemistry* 2(6): 128-135 (2014).

[15] J. O. Babalola, J. O. Olowoyo, A. O. Durojaiye, A. M. Olatunde, E. I. Unuabonah, M. O. Omorogie, Understanding the removal and regeneration potentials of biogenic wastes for toxic metals and organic dyes. *Journal of Taiwan Inst Chem Eng* 58:490–499 (2016).

[16] J. Zhong, J. Zhou, M. Xiao, J. Liu, J. Shen, J. Liu, S. Ren, Design and syntheses of functionalized copper-based MOFs and its adsorption behavior for Pb (II). *Chinese Chemical Letters*, 33(2): 973-978 (2022).

[17] D. K. dos Santos, R. Treméa, E. Lorençon, P. Rodrigues Batista, L. A. de Almeida Coral, B. de Jesus, F. Bassetti, Removal of Methyl Violet Dye by Adsorption Process on Hydrogen Titanate Nanotubes: Experimental-Theoretical Study. *Water, Air, & Soil Pollution*, 233(5): 1-15 (2022).

[18] N. Abdus-Salam, S. K. Adekola, Biosorption of Dyes. *App. Water Sci.*, 28-222. https://doi.org/10.1007/s13201-018-0867-7 (2018).

[19] F. O. Nwosu, F. A. Adekola, A. O. Salami, Adsorption of N-nitrophenol (PNP) Using Pilli nut shell action. *Pak. J. Anal. Environ. Chem.* 18 (1): 69. https://doi.org/10.21743/pjaec/2017.06.07 (2017).

[20] M. Harja, G. Buema, D. Bucur, Recent advances in removal of Congo Red dye by adsorption using an industrial waste. *Scientific Reports*, 12(1): 1-18 (2022).

[21] S. Lee, J. Park, S. Kim, S. Kang, J. Cho, J. Jeon, Y. Lee, D. Seo, Sorption Behavior of Malachite Green onto Pristine Lignin to Evaluate the Possibility as a Dye Adsorbent by Lignin. *Applied Biological Chemistry*, 62(37):1-10 (2019)

[22] B. S. Yadav, S. Dasgupta, Effect of time, pH, and temperature on kinetics for adsorption of methyl orange dye into the modified nitrate intercalated Mg/Al LDH adsorbent. *Inorganic Chemistry Communications*, 109203 (2022).

[23] T. Liu, Y. Lawluvy, Y. Shi, J. O. Ighalo, Y. He, Y. Zhang, P. S. Yap, Adsorption of cadmium and lead from aqueous solution using modified biochar: a review. *Journal of Environmental Chemical Engineering*, 10(1):106502 (2022).

[24] A. M. Ayuba, M. Ladan, A. S. Muhammad, Thermodynamic and kinetic study of Pb(II) amputation by river sediment. *Appl. J. Envir. Eng. Sci*. 6(3): 213-226 (2020).

[25] C. Kamatchi, S. Arivoli, R. Prabakaran, Thermodynamic, Kinetic, Batch Adsorption and Isotherm Models for the Adsorption of Nickel from an Artificial Solution Using Chloroxylon Swietenia Activated Carbon. *Physical Chemistry Research*, 10(3): 315-324 (2022).

[26] M. R. R. Kooh, R. Thotagamuge, Y. F. C. Chau, A. H. Mahadi, C. M. Lim, Machine learning approaches to predict adsorption capacity of Azolla pinnata in the removal of methylene blue. *Journal of the Taiwan Institute of Chemical Engineers*, 132: 104134 (2022).

[27] M. E. Gonzalez-Lopez, C. M. Laureano-Anzaldo, A. A. Perez-Fonseca, M. Arellano, J. R. Robledo-Ortiz, A critical overview of adsorption models linearization: methodological and statistical inconsistencies. *Separation & Purification Reviews*, 51(3): 358-372 (2022).

[28] M. S. Yahia, A. S. Elzaref, M. B. Awad, A. M. Tony, A. S. Elfeky, Efficient adsorption of chlorpyrifos onto modified activated carbon by gamma irradiation; a plausible adsorption mechanism, *Zeitschrift für Physikalische Chemie*, 236(1): 1-25 (2022).

[29] G. Mckay, H. S. Blair, J. R. Gardiner, The adsorption of dyes onto chitin in fixed bed column and batch absorbers. *Journal of Applied Polymer Science,* 29(5):1499-1514 (1984).

[30] F. Zhou, G. Ye, Y. Gao, H. Wang, S. Zhou, Y. Liu, C. Yan, Cadmium adsorption by thermal-activated sepiolite: Application to in-situ remediation of artificially contaminated soil. *Journal of*

*Hazardous Materials*, 423: 127104 (2022).

[31] M. Gao, Y. Zhou, J. Yan, L. Zhu, Z. Li, X. Hu, X. Zhan, Efficient precious metal Rh (III) adsorption by waste P. pastoris and P. pastoris surface display from high-density culture. *Journal of Hazardous Materials*, 427: 128140 (2022).

[32] T. Smith, T. Santhi, A. L. Prasad, S. Manonmani, *Cucumis Sativus* used as adsorbent for the removal of dyes from aqueous solution. *Arab. J. Chem*. 10: S244–S251 (2017).

[33] O. Golubyatnikov, E. Akulinin, Application of the Dubinin–Radushkevich–Astakhov equation to calculate gases isotherms on zeolite adsorbents (on example of $H_2$, $CO_2$, CO, $CH_4$, $N_2$ adsorption on 13X and 5A). *Separation Science and Technology*, 1-14 (2022).

[34] E. R. Ushakumary, G. Madhu, Removal of cadmium, chromium, copper, lead, and zinc ions by Alisma plantago aquatica. *International Journal of Environment and Waste Management* 13(1): 75-89 (2014).

[35] K. Sumanjit, T. P. S. Walia, Use of Dairy Sludge for the Removal of Some Basic Dyes. *Journal of Environmental Engineering and Science*. 7 (5): 433-438 (2008).

[36] E. Akar, A. Altinisik, Y. Seki, Using of activated carbon produced from spent tea leaves for the removal of malachite green from aqueous solution. *Journal of Ecological Engineering*. 52:19– 27 (2013).

---

(2022) ; www.mocedes.org/ajcer